# The development of a standalone computer simulation tool for the optimization of gypsum recovery at Afmine

by C. Maree*, A.J. Burger*, and C. Aldrich*

**Paper written on project work carried out in partial fulfilment of B.Eng (Chem. Eng.)**

**Synopsis**

**This paper describes the development and use of a process simulator to optimize gypsum recovery at Afmine, a small plant near Yzerfontein on the South African West Coast. The simulator consisted of models of the major plant equipment, viz. hydrocyclones, surge bins, settling tanks, a primary sieve and a dewatering screen. Experimental data suggested that the equipment could be modelled satisfactorily from data published in the open literature. Simulation studies have indicated that gypsum losses on the plant could be reduced substantially by means of some relatively minor modifications to the plant layout. Moreover, sensitivity analyses of the plant have indicated that optimization of the settling tanks should receive priority over the other process units.**

## Introduction

At least 90 per cent of the gypsum produced in the world is used in the building industry. In its uncalcined state it is universally used as a retarder in Portland cement and most South African production is used for this purpose. The mineral is added as small lumps to the cement clinker before grinding. Plaster of Paris is used for stuccowork, ornamental mouldings, and heat and sound insulating plasters. Gypsum board, which is extensively used in prefabricated houses, consists of one or more layers of gypsum sandwiched between sheets of unsized paper or other material.

Furthermore, plaster of Paris is widely used in industry, medicine, dentistry, and the arts for making moulds and casts. Keene's cement is used for hard-finish wall plasters and ornamental plasterwork generally. Building material gypsum products have the major advantages of not warping and being both fire resistant and vermin proof.

Raw gypsum is used extensively in many countries as a soil conditioner and in the manufacture of sulphuric acid and ammonium sulphate. Finely ground, it is known as 'mineral white' and is used as filler, for example in the paint industry. Less important uses are as a flux in metallurgy, and for conditioning water used in breweries. Alabaster has been used since ancient times for making vases, bowls and other ornamental objects. Soluble anhydrite is an all-purpose drying agent.

In contrast to gypsum deposits in other parts of the world, which were normally formed as chemical precipitates from marine water of high salinity, those in South Africa have mainly formed near the surface. Afmine is a small gypsum recovery facility, situated near Yzerfontein in the Western Cape district. Yzerfontein is well known for its gypsum deposits, and some 1.8 million tons of ore are available in two large salt pans. The average concentration of $CaSO_4{\bullet}2H_2O$ (gypsum) in this ore is 80%. Afmine uses one of these resources for the extraction of gypsum. A dredger is permanently situated in the salt pan, from where the gypsum is transported to the facility. Effluent from the plant is simply discharged into the same salt pan, as it has not been contaminated in any way.

The surface area of the salt pan is strongly influenced by the seasonal rains. In the winter when rainfall is high, the pan is filled with water from the pan's drainage area. Mining is done on the outskirts of the pan, where the dredger's drill can reach the gypsum. In summertime, the pan empties owing to high levels of evaporation and the dredger has to be moved deeper into the pan to prevent being marooned on dry land. Mining is subsequently done on the newly formed edge of the pan.

From the dredger, the slurry enters a surge bin through a primary screen, which removes oversize gypsum particles (called flakes). The flakes are stockpiled and left to dry. The underflow from the screen reports to the surge bin, which operates as a simple settling vessel. The overflow of this vessel is considered to be

* *Department of Process Engineering, University of Stellenbosch, Matieland.*

 *SA ISSN 0038–223X/3.00 + 0.00. Paper received Feb. 2005; revised paper received Feb. 2005.*

poor in gypsum and is returned to the salt pan. The underflow is treated by sending it through a series of hydrocyclones, settling tanks, and a linear screen in succession, as shown in Figure 1.

## Improvement of plant operations

Analysis of the tailing stream showed that approximately 30% of incoming gypsum is lost by returning it to the salt pan. It is believed that almost half of this portion can be recovered without excessive cost. The goal of the project was to develop a simulation tool that could be used to simulate process operations and to use these models to evaluate different plant configurations and operating parameters within the constraints of the existing equipment and layout. This would allow engineers to examine the process by altering process parameters such as equipment size or operating conditions. With the simulator, the gypsum recovery is then calculated, while the user is able to change various parameters such as flow rates, solids, contents and particle size distribution to explore the effect of these modifications on plant performance.

Part of the objective was also that the software had to be simple to use, self-explanatory and reliable in its calculations. Easily interpretable output had to be given as to what the expected behaviour of the plant would be, given the selected parameters. Moreover, the package had to be sufficiently flexible to be used as a practical tool for training staff in the operation of Afmine.

## Simulation of gypsum recovery process

### *Hydrocyclone*

The hydrocyclone plays an important role in the process used at Afmine, as indicated by the process flowsheet shown in Figure 1. Among the many models proposed to estimate the cut size of a cyclone, the one proposed by Plitt[1] provides accurate predictions over a wide range of operating conditions and design parameters. The model has been successfully applied to the development of automatic control systems in the comminution circuits of various Australian mines and was therefore used in the simulator.

It gives the cut size ($d_{50}$) as

$$d_{50} = \frac{14.8 \cdot D_c^{0.46} \cdot D_i^{0.6} \cdot D_o^{1.21} \cdot \exp(0.063 \cdot V)}{D_u^{0.71} \cdot h^{0.38} \cdot Q^{0.45} \cdot (S-L)^{0.5}} \quad [1]$$

The volumetric flow rate of slurry ($Q$) to the cyclone can be calculated as follows[2]:

$$Q = \frac{0.53 \cdot P^{0.56} \cdot D_c^{0.21} \cdot D_i^{0.53} \cdot h^{0.16} \cdot \left(D_u^2 + D_o^2\right)^{0.49}}{\exp(0.0031 \cdot V)} \quad [2]$$

Likewise, the pressure drop ($P$) can be calculated by rearranging [2]:

$$P = \frac{1.88 \cdot Q^{1.78} \cdot \exp(0.005 \cdot V)^{0.49}}{D_c^{0.37} \cdot D_i^{0.94} \cdot h^{0.28} \cdot \left(D_u^2 + D_o^2\right)^{0.87}} \quad [3]$$

The amount of water that goes to the underflow is a measure of the solids in the feed that bypass the cyclone without being classified, while [4] is a measure of the pulp that bypasses the cyclone:

$$s = \frac{34.4 \cdot \left(D_u / D_o\right)^{3.31} \cdot h^{0.54} \cdot \left(D_u^2 + D_o^2\right)^{0.36} \cdot \exp(0.0054 \cdot V)}{(dP)^{0.24} \cdot D_c^{1.11}} \quad [4]$$

However, [4] is only valid when there is a free discharge of both the overflow and underflow, since siphoning and back pressure may render it invalid.

The fraction of the pulp in the feed reporting to the underflow, given by [5] and [6] in SI units[2], serves as a measure of the sharpness of classification, with $m$ (Rossin-Rammler sharpness of separation value) representing the slope of the Tromp curve[3]. Large values of $m$ represent sharp classification. Classification is considered to be sharp for a value of $m$ exceeding 3, while a value of less than 2 is considered to represent poor classification.

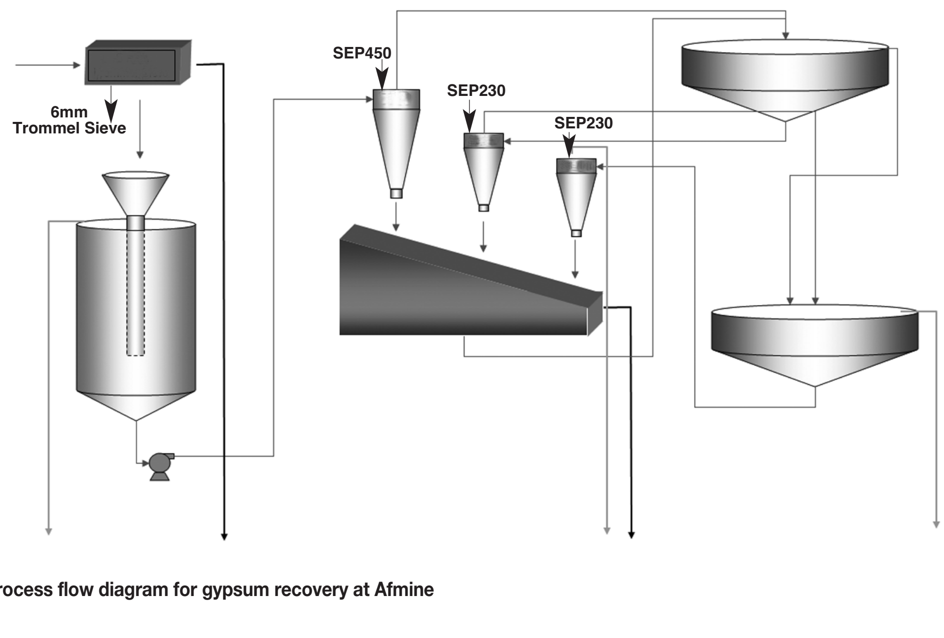


**Figure 1—Current process flow diagram for gypsum recovery at Afmine**

$$R_v = \frac{S}{S+1} \quad [5]$$

$$m = 2.96 \cdot \exp\left(-1.58 \cdot R_v\right) \cdot \left(\frac{D_c^2 \cdot h}{Q}\right) \quad [6]$$

Finally, Plitt has shown that the corrected classification curve can be represented by a Rosin-Rammler type probability Equation [7].

$$E_C = 1 - \exp\left[-0.6931 \cdot \left(\frac{d}{d_{50}}\right)^m\right] \quad [7]$$

The corrected probability is defined as the probability of particles of a given size ($d$) that will report to the underflow as a result of classification.

### Settling tank

Another important vessel in Afmine's process is the settling vessel. When many particles flow in a fluid in close proximity to each other, the motion of each particle is influenced by the presence of the others and a simple analysis of single particle settling is no longer valid.

For a suspension of particles in a fluid, Stokes's law [8] relating the terminal velocity of a single particle in the fluid to the particle size, particle and fluid densities and fluid viscosity may be assumed to apply. The fundamentals of settling rates of particles suspended in a fluid are based upon a simple force balance on each particle, i.e. drag force = weight–upthrust.

$$U_{T,O} = \frac{d_p^2 \cdot \left(\rho_s - \rho_f\right) \cdot g}{18 \cdot \mu} \quad [8]$$

Equation [8] should now be altered to comply with hindered settling, since the force balance is valid for a single particle only. This is done by multiplying terminal velocity of the article ($U_T$) by the volumetric fraction of the solids, raised to a power '$n$'.

The fluid in which the particles are suspended is assumed to be pure water. This assumption may have to be revisited in more sophisticated versions of the model, since the water has a relatively high total dissolved solids (TDS) count. The theoretical settling rate should be somewhat lower than the true settling rate, because of the higher actual fluid density. This lower true settling velocity was accounted for by incorporating a reasonable safety factor into the model.

The density of pure water was estimated by [9]

$$\rho_l = 1000.580427 - 0.0932831 \cdot T - 0.003424212 \cdot T^2 + 0.0000018606 \cdot T^3 \quad [9]$$

Similarly, the fluid viscosity was estimated by [10]

$$\mu = \frac{1749.4 - 53.31 \cdot T + 0.93 \cdot T^2 - 0.00705 \cdot T^3}{1000000} \quad [10]$$

Finally, the data in Table I was used to account for the free fall orientations of the particles and the effect this had on the drag, and ultimately the hindered settling velocity of the particles.

When working with terminal velocities of small particles, it is safe to assume low Reynolds numbers (Re < 5.5) and hence stable particle orientations. Nonetheless, one should still compensate for the possible non-sphericity of the particles.

The sphericity constant (K) is used to adapt the terminal settling velocity of a particle in such a way as to correct for non-spherical particles. The sphericity of the gypsum particles (in this case approximately 0.7, from data obtained via image analysis of the particles) was estimated by [11][4].

$$K = 0.843 \cdot Log\left(\frac{\varphi}{0.065}\right) \quad [11]$$

The factor '$n$' is used to calculate the hindered settling velocity in a settling vessel. In order to obtain '$n$', one has to evaluate the Archimedes number representative of the particle-fluid system. This dimensionless number can be calculated using [12][5].

$$Ar = \frac{d_p^3 \cdot \rho_l\left(\rho_s - \rho_l\right)g}{\mu^2} \quad [12]$$

Once calculated, the Archimedes number is used to determine $n$, as shown in [13][5].

$$\frac{4.8-n}{n-2.4} = 0.0043 \cdot Ar^{0.57} \cdot \left[1 - 2.4\left(\frac{d_p}{D}\right)^{0.27}\right] \quad [13]$$

The hindered settling rate of a particle size is obtained by initially evaluating Equation [7] (for settling of a single particle), followed by [11] (sphericity). These two quantities may be used to obtain the hindered settling rate for non-spherical particles, as shown in [14].

$$U_T = U_{T,0} \cdot K \cdot \varepsilon^n \quad [14]$$

### Dewatering screen

Models for linear screens are not widely published. Companies like Delkor and Linatex have done considerable research on linear screens, but unfortunately their findings are considered propriety knowledge. Ruhmer[6] has published a method used to estimate the behaviour of a linear screen.

Ruhmer[6] defines the efficiency of a linear screen as the ratio of the undersize obtained in screening to the amount of undersize available in the feed [15].

$$E = \frac{100 \cdot (e - v)}{e \cdot (100 - v)} \quad [15]$$

When [15] is rearranged, solving for $v$, [16] is obtained.

*Table I*

**Free fall orientations of particles[4]**

| Reynolds number | Orientation |
|---|---|
| 0.1–5.5 | All orientations stable |
| 5.5–200 | Stable in position of maximum drag |
| 200–500 | Unpredictable: disks and plates tend to wobble while fuller bodies tend to rotate |
| 500–200000 | Rotation about axis of least inertia; frequently coupled with spiral translation |

$$v = \frac{100 \cdot e(1-E)}{(100 - E \cdot e)} \quad [16]$$

This equation is used, along with an estimated efficiency to approximate the amount of undersize reporting to the overflow. E is estimated using Table II, provided by Ruhmer[6].

The efficiency of the Linatex linear screen at Afmine was estimated by use of a 5th order polynomial fitted to the data given in Table II. Once the efficiency has been estimated, and the per cent undersize reporting to the overflow has been calculated using [16], one need only apply a mass balance over the screen. This will determine the overflow and underflow flow rates and solid percentage.

The particle size distributions for the overflow and underflow cannot be calculated using such a rudimentary calculation. A more sophisticated model is required, the likes of which are not readily attainable in the literature. Such models are available to large companies who have directed research in the specific area.

The screen area required is calculated using a model provided by Ruhmer[6].

$$Area = \frac{(TF - OS)}{A \cdot B \cdot C \cdot D \cdot E} \quad [17]$$

The constants A to D are determined using the same technique as described for that of E. Similar graphs were constructed for constants A through D, and the equations describing them are summarized in Table III.

## Implementation

The executable program was written in an object-based programming language, providing a user-friendly graphic user interface (GUI). In basic terms, the GUI is the main operating screen of the project. It seemed appropriate to present the user with a flowsheet of the process. Each image of a unit on this interface acts as a link, which opens a form containing essential information about the unit. In this form, the user may alter various parameters, such as the size of the unit or the feed conditions. It also communicates specialized information not generated in the final report, such as information regarding the unit, or the particle size distribution (PSD) at that specific point in the process. Figure 3 shows a screen shot of the main GUI.

The development of the main screen is done by opening a new project in Delphi. A form is opened, which is set as the main form. After resizing the form, the image of the flowsheet is pasted on the background. A clickable surface is created on each unit in the form of an empty image box. Each image box will lead to a different form being opened when the user clicks on it. 'Edit' boxes have been inserted next to the flow lines on the diagram. These boxes contain the flow rates and solid percentages of the specific pipeline. Two buttons were inserted, labelled 'Simulate' and 'Report' for the purpose of initiating the simulation, and generating the final report. The menu bar was inserted next, which contains the drop-down menus for 'File', 'Misc' and 'Help'. Every separate unit form presents the user with a photograph of the unit, among others to help trainees better relate to the actual system.

This basic procedure is followed for each unit in the flowsheet. Every unit is assigned its own form, and a photograph of the unit is added to the background. Various specialist functions are built into each unit. The user has the option to either first alter some or all the parameters, or run a simulation using default values. After a simulation has been completed, a report may be generated by clicking on the 'Report' button. Data can also be saved to a file for later use, or may be called upon from a previously saved file.

## Verification of the simulator

Although the overall behaviour of the simulator was not validated, its ability to model the individual units was tested experimentally, as discussed below.

### *Primary sieve*

The model representing the primary sieve appeared to be reasonably accurate. Experimental data have indicated that 12% of the incoming particles reported to the overflow, while the model predicted that 11% would report to the overflow. Moreover, the predicted particle size distribution was cut

*Table II*

**Estimation of the efficiency of a linear screen[6]**

| Aperture (mm) | 0.8 | 1.5 | 2.0 | 3.2 | 3.4 | 4.8 | 6.4 | 7.9 | 9.5 | 12.7 | 19.0 | 25.4 |
|---|---|---|---|---|---|---|---|---|---|---|---|---|
| Efficiency, E | 1.1 | 1.4 | 2.0 | 2.5 | 2.5 | 2.5 | 2.3 | 2.0 | 1.5 | 1.3 | 1.2 | 1.1 |

*Table III*

**Constants A to E used in [16]**

| Parameter | Model | Variable *x* | Units of *x* | Parameter value |
|---|---|---|---|---|
| A | $0.8181x + 2.8485$ | Aperture | mm | 0.9834 |
| B | $-0.0002x^2 + 0.0101x + 0.8862$ | Percentage oversize in feed | % | 0.9045 |
| D | $0.4434 \exp(0.0203x)$ | Amount of feed less than half the aperture | % | 0.9935 |
| E | $1E{-}05x^5 - 0.001x^4 + 0.0261x^3 - 0.321x^2 + 1.5795x - 0.0975$ | Aperture | mm | 0.9735 |

Note: The value of C is assumed to be 1.7. All other parameters have been determined by least squares estimates from experimental data.

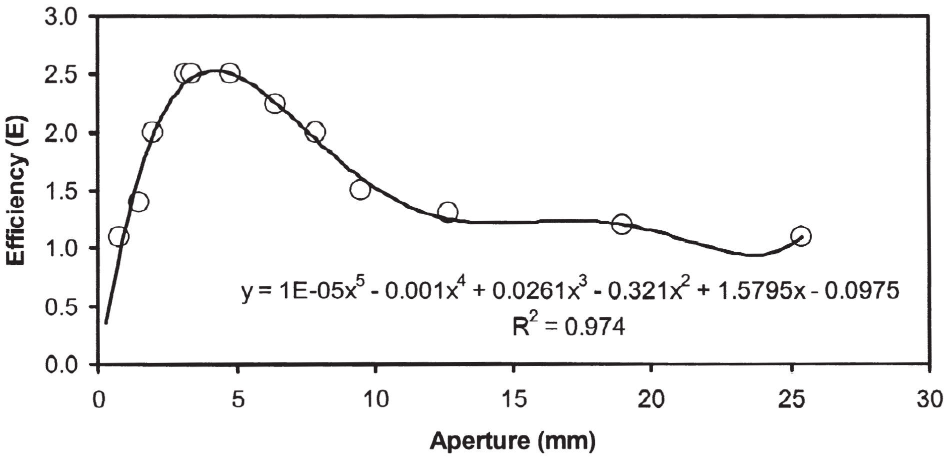


**Figure 2—Estimation of the efficiency for the linear screen**

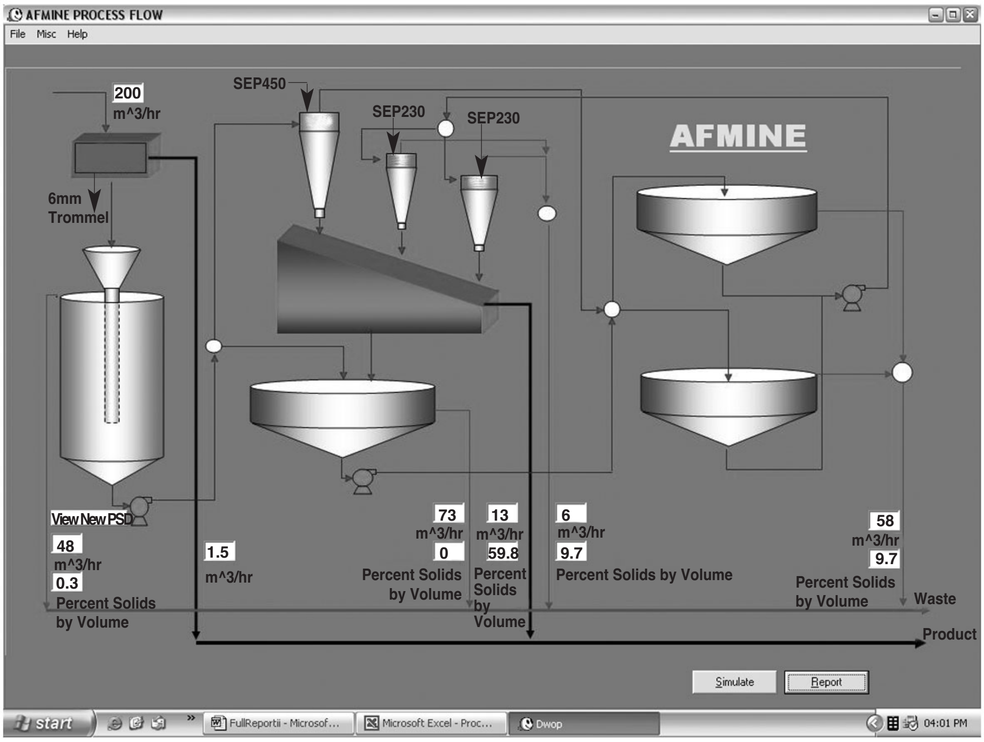


**Figure 3—Screenshot of the graphic user interface (GUI) of the simulation software**

sharply, allowing for some 10% (depending on the feed flow rate) undersize particles to report to the overflow. The experimental data confirmed this approximation.

### *Surge bin*

Likewise, the model predicting the performance of the surge bin appeared to be reliable. It predicted more efficient classification than the experimental results suggested, since the model simulated the behaviour of a surge bin with a submerged feed line, while the experiments were done on a vessel operating with a surface feed. The experimental unit experienced bypassing of solids, while the theoretical unit simulated optimized results. The reason for simulating an improved unit was to prove the relevancy of the proposed alteration on the process (submerging the feed).

### *Settling tanks*

The model was found to represent the actual process satisfactorily. It predicted a slightly lower overflow solids percentage, which was justified by the lower incoming percentage of fine solid percentage. The experiments showed a sharper cut, owing to the partially submerged feed, with a feedwell. The feedwell prohibits bypassing of particles directly to the overflow.

### *Hydrocyclones*

The model predicted better performance than was suggested by the experimental data. The model is, however, accepted as satisfactory, as the cyclone that was tested, might not have been operating at its optimal efficiency, as assumed by the model. One of the reasons for this is that the cyclone that was tested had been exposed to normal wear and tear over a substantial period.

### *Dewatering screen*

The model predicted the percentage of overflow solids as 69% by mass and the area required to attain this overflow as 5.02 $m^2$. In contrast, the experimental data indicated the percentage of overflow solids to be 63% by mass and the commensurate area to be 4.68 $m^2$. Again the model appears to behave satisfactorily, since enlarging the surface area will improve separation.

## Discussion and results

The simulation software was used to assess various scenarios. As an example, Figure 4 shows a process flow diagram alternative to the one representing current plant operations. The two flowsheets are similar, except for the introduction of a closed circuit recycle loop in the alternative flowsheet shown in Figure 2.

### *Flowsheet improvement*

By running various simulations, the alternative flowsheet could be improved by reducing the sizes of the the second and third cyclones, as well as by adding a third settling vessel. In addition, a recycle structure was added to prolong the residence time of each particle. This recycle loop runs between the three hydrocyclones, the dewatering screen and the three settling vessels.

Figure 10 shows a screenshot of the program with an open window containing the generated report. The report is generated in a user-friendly style, and the user has the option of printing the generated report to the default printer.

A number of other simulations were run to test various hypotheses. For example, it was found that when the underflow rates in the settling tanks were increased, the recovery improved dramatically. This underscored the previous conclusion that the cyclones were somewhat oversized.

Moreover, simulations have shown that running settling vessels 2 and 3 in parallel, will reduce the upward flow in the tank and therefore reduce the particle size that is discarded. It can also work the other way around in that one can now use smaller vessels and obtain the same cut-point. The same line of reasoning applies to cyclones 2 and 3, which are also run in parallel. They are significantly smaller than the first cyclone, because they treat a much lower flow rate.

In conspectus, the simulations suggested that the improved process design could increase the overall recovery of gypsum significantly, especially owing to the inclusion of an enlarged recycle structure. Also, the parallel flow of slurry through two settling vessels and two small hydrocyclones causes the total flow per unit to be halved. This has a positive effect on the settling vessels, since a smaller flow will result in a smaller upward slurry velocity. This in turn will lower the cut-point of the vessel, meaning less gypsum will be returned to the salt pan.

### *Sensitivity analysis*

A sensitivity analysis was carried out with the software in order to determine which of the units has the largest influence on the operation and efficiency of the plant. Table IV summarizes the effect of the various units in the plant. Each unit was assigned a sensitivity rating between 1 and 6. A sensitivity rating of 1 means that altering the unit's size has the least influence on the process, while a sensitivity rating of 6 means that altering the unit's size has the largest influence on the process.

The dewatering screen has the largest influence on the process, and it is recommended that this unit should be the first to be optimized.

## Current limitations of the simulator

At present the simulator is limited by (a) the assumption that

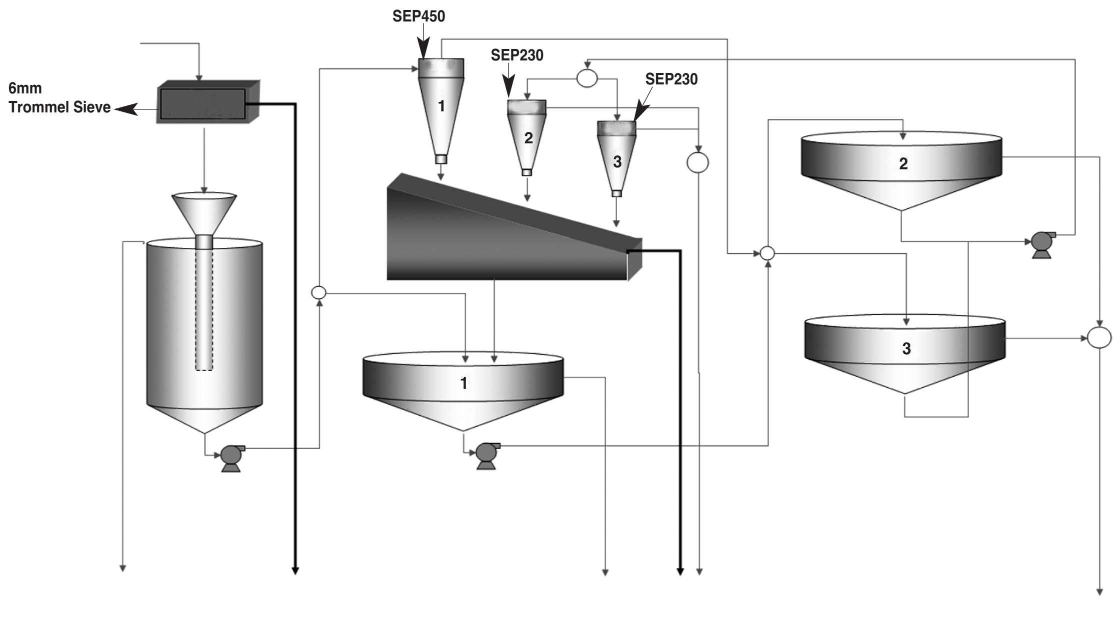


**Figure 4—Alternative process flow diagram for gypsum recovery at Afmine**

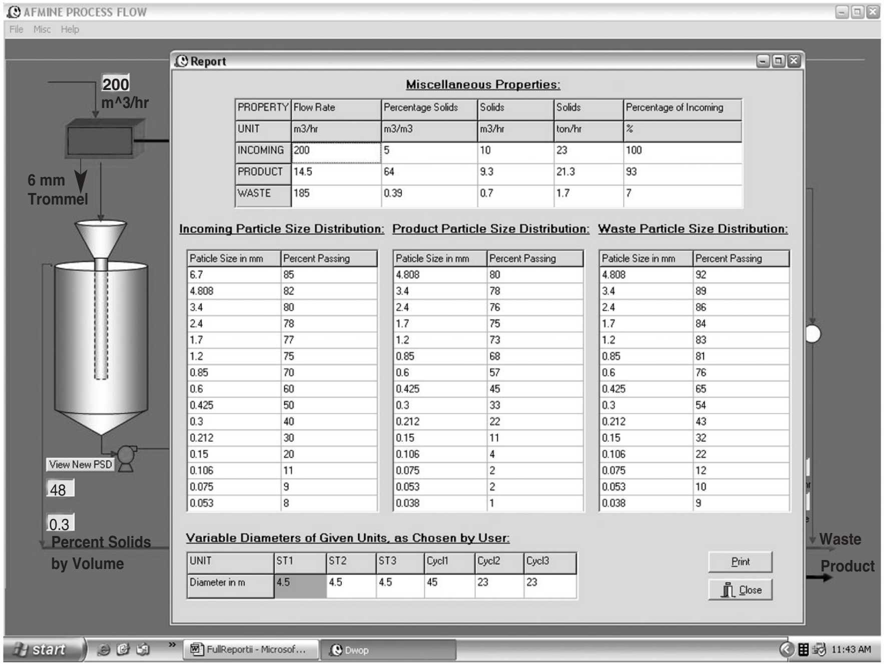


**Figure 5—Screenshot of the generated report**

*Table IV*

**Sensitivity of each unit, sorted in ascending priority**

| Unit | Sensitivity rating |
|---|---|
| Settling tank number 1 | 1 |
| Settling tank number 2 | 2 |
| Settling tank number 3 | 2 |
| Hydrocyclone number 2 | 3 |
| Hydrocyclone number 3 | 3 |
| Hydrocyclone number 1 | 4 |
| Surge bin | 5 |
| Dewatering screen | 6 |

the process water is assumed to be pure, (b) the model for the dewatering screen is limited, and (c) the process flowsheet is fixed, i.e. units cannot be moved or removed automatically.

Of these, the assumption of process water being pure water should not have a major implication on the process results. It will provide a slightly optimistic result as it assumes a smaller liquid-solid density difference than is observed in practice.

The simplified model used for the dewatering screen may pose a problem if drastic changes are made in the operating conditions. The present model is not specific, but does account for area, aperture size and load rate. Further research would therefore be needed to improve this model.

The fixed process flowsheet has the implication that the model can be used only for the specific layout of the plant. Altering the flowsheet or using this model for a different flow layout, will provide worthless data.

## Summary

An inexpensive simulator based on models mostly published in the open literature was developed to analyse the recovery of gypsum in a small plant. Experimental data suggested that the models for a primary sieve, surge bin, hydrocyclones, settling tanks and a dewatering screen represent plant behaviour satisfactorily. Simulation of alternative plant layouts suggested that current gypsum losses could be reduced dramatically without undue cost.

A sensitivity analysis of the process circuit has indicated that the largest gains would be obtained by improving the performance of the settling tanks, while the operation of the surge bins and dewatering screen was least important.

## Acknowledgements

Afmine's support of the project is gratefully acknowledged.

## Nomenclature

| Symbol | Description | Units |
|---|---|---|
| Ar | Archimedes number | [-] |
| Area | Dewatering screen area | [$m^2$] |
| B | Constant used in equation 17 | [-] |
| C | Constant used in equation 17 | [-] |
| D | Constant used in equation 17 | [-] |
| $d_{50}$ | Cyclone cut-size | [μm] |
| $d_p$ | Particle diameter | [m] |
| $D_c$ | Inside diameter of cyclone | [cm] |
| $D_i$ | Inside diameter of inlet | [cm] |
| $D_o$ | Inside diameter of vortex finder | [cm] |
| $D_u$ | Inside diameter of apex | [cm] |
| E | Efficiency of a linear screen | [%] |
| e | Linear screen's undersize in the feed | [%] |
| $E_c$ | Plitt's corrected probability | [-] |

| | | |
|---|---|---|
| g | Gravitational acceleration | [m/s2] |
| h | Distance from bottom of vortex to top of underflow orifice (free vortex height) | [cm] |
| K | Sphericity constant | [-] |
| L | Density of liquids | [kg/m3] |
| m | Sharpness of separation | [-] |
| n | Constant in Equation [13] | [-] |
| OS | Mass of feed that is smaller than the apertures | [ton/hr] |
| P | Pressure drop across cyclone | [kPa] |
| Q | Flow rate of feed slurry | [m3/h] |
| $R_v$ | Fraction of pulp reporting to the underflow | [-] |
| S | Density of solids | [g/cm3] |
| s | Volumetric distribution of pulp | [-] |
| T | Temperature | [C] |
| TF | Total feed to the dewatering screen | [ton/hr] |
| $U_{T,0}$ | Stokes's settling rate | [m/s] |
| $U_T$ | Hindered settling rate | [m/s] |
| V | Volumetric percentage solids in the feed | [%] |
| $v_r$ | Radial velocity of particle | [rad/s] |
| $v$ | Linear screen's undersize in the overflow | [%] |
| $\mu$ | Viscosity of suspending medium | [kg/m.s] |
| $\omega$ | Angular velocity | [rad/s2] |
| $\rho_s$ | Density of solids | [kg/m3] |
| $\rho_1$ | Density of suspending liquid | [kg/m3] |
| $\varphi$ | Sphericity of a particle | [-] |

## References


1. PLITT, L.R. A mathematical model of the hydrocyclone classifier. *CIM Bulletin*, 1976. pp. 114–123.
2. CONWAY, T.M. *A Computer Programme for the Prediction of Hydrocyclone Performance, Parameters, and Product Size Distributions*, MINTEK, South Africa, Counsil for Mineral Technology, 1985.
3. SVAROVSKY, L. *Hydrocyclones*, Holt Rinehart and Winston Ltd., England. 1984.
4. PERRY, R.H. AND GREEN, D.W. *Perry's Chemical Engineers' Handbook*, McGraw-Hill Professional, 7th ed, ISBN 0070498415, 1997.
5. RHODES, M.J. *Introduction to Particle Technology*, John Wiley & Sons, United Kingdom, 1998.
6. RUHMER W.T. *Handbook on the Estimation of Metallurgical Process Costs*, MINTEK, South Africa, 1996. ◆